Deep-Sea Research II 50 (2003) 2997–3015

DEEP-SEA RESEARCH
PART II

www.elsevier.com/locate/dsr2

Remote sensing and surface POC concentration in the South Atlantic

Alexey V. Mishonov*, Wilford D. Gardner, Mary Jo Richardson

Department of Oceanography, Texas A&M University, College Station, TX 77843-3146, USA

Received 30 April 2002; received in revised form 31 March 2003; accepted 15 July 2003

Abstract

Several SeaWiFS products have been compared with shipboard data to assess the possibility of using remote sensing to estimate particulate organic carbon (POC) concentration in surface waters. Transmissometer data were collected during six South Atlantic Ventilation Experiment (SAVE) hydrographic expeditions conducted between November 1987 and March 1989 from R/V *Knorr*, and *Melville*. A total of 361 beam attenuation profiles were made with a SeaTech transmissometer interfaced with a CTD/rosette. In order to calculate the POC concentration from transmissometer profiles, a regression between beam attenuation and POC for open Atlantic Ocean waters derived from our research in the North Atlantic (North Atlantic Bloom Experiment, NABE) and enhanced by data from the Bermuda Atlantic Time Series Station (BATS) was applied. The profiles were processed and examined as vertical sections of the surface 250 m. The data were collected in two successive years, during the same season, which allowed us to compile a combined data set over the austral summer for examination. Beam attenuation/POC concentrations were integrated down to one attenuation depth with the intent of making comparisons with satellite optical data. No satellite optical data were available for 1987–1989, so the only option was to compare our integrated data with SeaWiFS-derived variables from later years averaged over the same season as SAVE data. Analysis of four SeaWiFS products acquired from 1997 to 2002 demonstrated very low variations from year to year for seasonally averaged data, suggesting that making comparisons of the beam attenuation/POC fields with averaged satellite optical products from later years is a valid (though not optimal) approach for this area. The highest correlation between beam attenuation/POC concentration and remotely derived products was found with normalized water-leaving radiance at 555 nm. Other SeaWiFS-derived variables—chlorophyll concentration, diffuse attenuation coefficient at 490 nm and integral chlorophyll (integrated over one attenuation depth)—were also compared but showed a slightly less satisfactory correlation.

1. Introduction

Data on particulate organic carbon (POC) concentrations over ocean-basin and global scales are sought to construct more complete carbon mass balances in the ocean and for validation of biological and biogeochemical models of carbon production and recycling. Some promising attempts at extracting POC concentration from SeaWiFS-derived reflectance at 555 nm were made recently in the Southern Ocean (Stramski et al., 1999). While this study was important as an

*Corresponding author. Tel.: +1-979-862-6674; fax: +1-979-845-6331.

E-mail address: avm@ocean.tamu.edu (A.V. Mishonov).

0967-0645/$ - see front matter © 2003 Elsevier Ltd. All rights reserved.
doi:10.1016/j.dsr2.2003.07.007

indication of a new approach, their results are based on limited data with small temporal and geographical range.

While POC determination from discrete bottle samples on a dense spatial grid would be a very labor and time demanding procedure, good estimates of POC distribution are possible when using in situ optical instruments (e.g., transmissometers) interfaced with a CTD. Data on the inherent optical property of beam attenuation can be related to the simultaneously obtained discrete samples of POC concentration at multiple depths and correlations derived. We have done this during all four of the JGOFS Process Studies (Gardner et al., 1993, 1995, 1999, 2000, 2003a, b; Chung et al., 1996, 1998; Gundersen et al., 1998; Morrison et al., 2001), and others have obtained similar results using bottle samples (Claustre et al., 1999). Similar work using large-volume in situ pumps to obtain POC values has been done by others (e.g., Bishop et al., 1999; Bishop, 1999). Correlations from pump samples, while showing a linear relation between beam attenuation and POC concentrations, can significantly underestimate the POC concentration in surface waters because the pump method does not retain all the POC (Dunne et al., 1997; Gardner et al., 2003a). Therefore, we use POC concentration obtained from bottle samples.

In order to expand our coverage to a global scale, we worked with many scientists to interface our transmissometers with the CTD on WOCE cruises during the last 15 years and archived the raw data. We also collected data during the South Atlantic Ventilation Experiment (SAVE) (Berglund, 1989; Gardner et al., 1990; SAVE, SIO Report, 1992; Wood, 1993) and other projects. We have been reducing and synthesizing the data during the last two years as part of the NSF-funded Synthesis and Modeling Project (SMP).

The purpose of this paper is to evaluate one application of our data from the SAVE program, namely to compare estimates of POC concentrations with satellite optical products. An advantage of the SAVE data is the coverage of the entire South Atlantic, which provides a wide dynamic range of oceanic conditions and POC concentrations. An important disadvantage, however, is that no ocean color satellites were operational during the SAVE study. Therefore, we first faced the question: is the interannual variability of satellite data small enough to allow us to reasonably compare ocean color products from an average of several years with POC concentration. To answer this question we compared SeaWiFS products (data reprocessing Version 4) for five consecutive years (1997–2002) to estimate the interannual spatial variability of four standard products. If averaged over the same season when SAVE data were collected (austral summer: December–April), the coherence from year to year is very good. It suggests that a comparison of our SAVE field data with satellite data collected a decade later, while not ideal, is still a reasonable approach for examining the data and attempting to produce a first-order algorithm from SeaWiFS data. Thus we can demonstrate the importance of this approach for future work when and where synchronous data can be obtained. Four SeaWiFS products were further examined to determine which one was best correlated with in situ derived POC data.

2. Methods

Transmissometer data were collected during six SAVE hydrographic expeditions conducted from the end of November 1987–April 1989 from R/V *Knorr* and *Melville* along lines shown in Fig. 1. A total of 361 beam attenuation profiles were made with a SeaTech transmissometer interfaced with a CTD/rosette. Data were initially reduced and partly reported by Berglund (1989), Wood (1993) and Gardner et al. (1990). An overview of the data processing is given below.

2.1. Beam c_p vs. POC relationship

Significant data processing and quality control were necessary to derive the finalized transmissometer data. Details of the methods in general are similar to those used previously (Gardner et al., 1993, 2003b, in revision; Gundersen et al., 1998) and during other JGOFS programs and briefly follow.

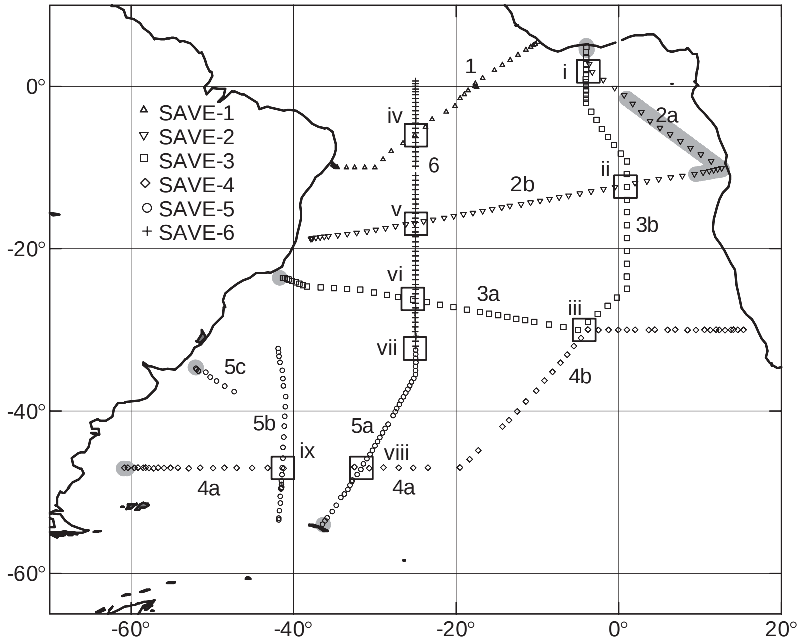

Fig. 1. Sampling grid for SAVE cruises. SAVE-1: 24 Nov–11 Dec 1987; SAVE-2: 19 Dec 1987–21 Jan 1988; SAVE-3: 29 Jan–06 Mar 1988; SAVE-4: 09 Dec 1988–13 Jan 1989; SAVE-5: 01 Feb–06 Mar 1989; SAVE-6: 14 Mar–08 Apr 1989. Boxes denote cruise crossings; gaps in the ship tracks are because no data were obtained in those locations. Gray shadow denotes the coastal areas with Case II waters.

The original raw light transmission data were sampled at high frequency (30 Hz), converted to beam attenuation (c), and were binned to a standard interval. The data reduction procedure was applied uniformly to all data and included: (a) filtering based on pressure; (b) spike removal using pressure-dependent filters and gradient checks; (c) averaging at 2 db intervals; and (d) examination and correction of remaining spikes, excessive noise, sensor trends or instrumental offsets. Air calibrations of each instrument were obtained before, during, and after each cruise according to the manufacturer's specifications (SeaTech, Inc., Bartz et al., 1978). Beam attenuation due to water (c_w) was subtracted from all data based on deep-water values. Our basic assumption has been that deep-waters are highly stable and constant in terms of hydro-optical characteristics. We used the minimum beam c values measured in deep-water as an absolute minimum value of every cruise. The manufacturer (Bartz, personal communication) has used this approach, and we (Gardner et al., 1985) have used it in modified ways during processing of the JGOFS transmissometer data to obtain beam c_p—beam attenuation due to particles. It is applicable as long as data from some stations in deep-water are collected (Gardner et al., 1993, 1995; Chung et al., 1996, 1998; Gundersen et al., 1998), as occurred during all SAVE cruises.

Water samples during SAVE cruises were collected and filtered to determine total particulate matter concentration (PM), but no samples were analyzed for POC. Because of biological variability the POC/PM ratio is not constant (Chung et al., 1996; Gardner et al., 2001), the PM data could not be used to derive a beam c_p/POC relationship. Therefore, to estimate the POC concentration based on SAVE beam attenuation data we used the beam c_p/POC regression from the North Atlantic Bloom Experiment (NABE; 165 data points) calculated by us earlier (Gardner et al., 1993; Mishonov et al., 2000) and modified by including additional data taken from Bermuda

Atlantic Time Series (BATS; 606 data points) archives (Gardner et al., 2001). Our choice to use these data was based on two main reasons: (a) the combined data set includes data covering a wide range of c_p/POC conditions from the intensive spring bloom (in the North Atlantic) to oligotrophic waters of a central Atlantic Gyre (BATS), and (b) there are no other concurrent c_p/POC data for the SAVE area that allow us to build a sound regional regression. From the NABE and BATS data we calculated a separate regression for each data set as well as a combined regression. First, we analyzed the BATS data by seasons and found only moderate seasonal variability (slopes: winter 0.0023 ± 0.0002, spring 0.0024 ± 0.0001, summer 0.0019 ± 0.0002, autumn 0.0015 ± 0.0002) over a moderate range of c_p (0.003–0.215). Second, we analyzed the differences between two separate regional regressions, the averaged regression and a regression based on the combined data set, and have considered the differences among them to be negligible (see Table 1). Therefore, we used the regression based on the combined data set in our analyses. Note that all linear regressions in this paper are Model II, where the errors in both X and Y are minimized simultaneously since both variables (POC and c_p) are measured quantities. We used 771 data pairs as a basis for the calculation, which produced the equation for c_p (m^{-1}):

$$c_p = \text{POC}\, 3.236 \times 10^{-3} - 1.333 \times 10^{-3},\quad n = 771,\ r = 0.94$$

or converting the equation for POC ($mg\, m^{-3}$):

$$\text{POC} = c_p\, 309.71 + 0.46, \quad n = 771,\ r = 0.94.$$

The last equation was used for the POC calculation for all six SAVE cruises.

2.2. Comparison with satellite data

The only totally valid sea-truthing of ocean-color data is with coincident data. Unfortunately no ocean color satellites were operating during the SAVE cruises (1987–1989). We postulated that the next best approach would be to compare ship-derived data with satellite ocean-color data obtained during the same months/seasons from years when satellite data were available. To validate this approach we used SeaWiFS ocean-color data products for the South Atlantic collected during the entire period of SeaWiFS operations (1997–2002) within the same months/seasons when SAVE data were acquired as will be described below.

Previous studies have shown that this approach can be used in areas where regular seasonal features or processes occur, such as the Amazon River outflow or quasi-stable frontal zones (Afonin et al., 1999—data for 1986–1990). In the South Atlantic potential areas of such phenomena include the Benguela Current off Southwest Africa, Congo River outflow, Sub-Antarctic front, South Equatorial Current, and Falkland Current, (Peterson and Stramma, 1991). All of these areas have high seasonal variability, but interannual cycles for such regions are fairly repeatable when averaged on seasonal/monthly time scales.

In this work we used global, equal-area grid data with resolution of 9 km (Level 3 Monthly data) collected from 1997 to 2002. Products

Table 1
Parameters of the linear regressions (Model II) between POC and c_p for NABE and BATS data sets

Parameters of the regression	Regional regressions (Model II)			
	NABE	BATS	Averaged regression	Combined data set
Slope	3.296×10^{-3}	3.094×10^{-3}	3.195×10^{-3}	3.236×10^{-3}
Intercept	-1.091×10^{-2}	3.063×10^{-3}	-3.923×10^{-3}	-1.333×10^{-3}
Slope SD	7.952×10^{-5}	8.517×10^{-5}	8.235×10^{-5}	3.899×10^{-5}
Intercept SD	7.147×10^{-3}	1.939×10^{-3}	4.543×10^{-3}	1.799×10^{-3}
R	0.951	0.735	0.843	0.942
n	165	606	—	771

analyzed were: (1) normalized water leaving radiance at 555 nm, $L_{WN}(555)$, (2) chlorophyll concentration, CHL, and (3) diffuse attenuation coefficient at 490 nm, K_{490}. Data files were obtained from the SeaWiFS data archives (http://daac.gsfc.nasa.gov/data/dataset/SEAWIFS/). Using the two last parameters we have calculated a fourth parameter: Integral Chlorophyll, i.e. chlorophyll integrated over one optical depth ($IC_K = CHL/K_{490}$) as suggested by Campbell et al. (1995).

Data for the study region (20°N, 65°S; 20°E, 70°W) were extracted from the global coverage data files. Spatial resolution was reduced from 9×9 (1×1 pixels) to $18 \times 18\,km^2$ (2×2 pixels) using SeaDas software (Baith et al., 2001). "No-data" values were eliminated, and data for five months (from December to April) were averaged in order to produce five seasonal compilations for austral summers of 1997–1998, 1998–1999, 1999–2000, 2000–2001, 2001–2002 and one five-year average for austral summer for each parameter. Averaged data were interpolated to a regular 0.5° grid, which was smoothed by averaging data within the nearest $1.5° \times 1.5°$ for each grid node. The resulting maps were compiled for every year. In this paper, due to obvious limitations, we have included only maps averaged over five years (Figs. 2a,b and 3a,b), but yearly maps are available for viewing/download at web-site: http://oceanography.tamu.edu/~pdgroup/DataDir/HTM_Files/

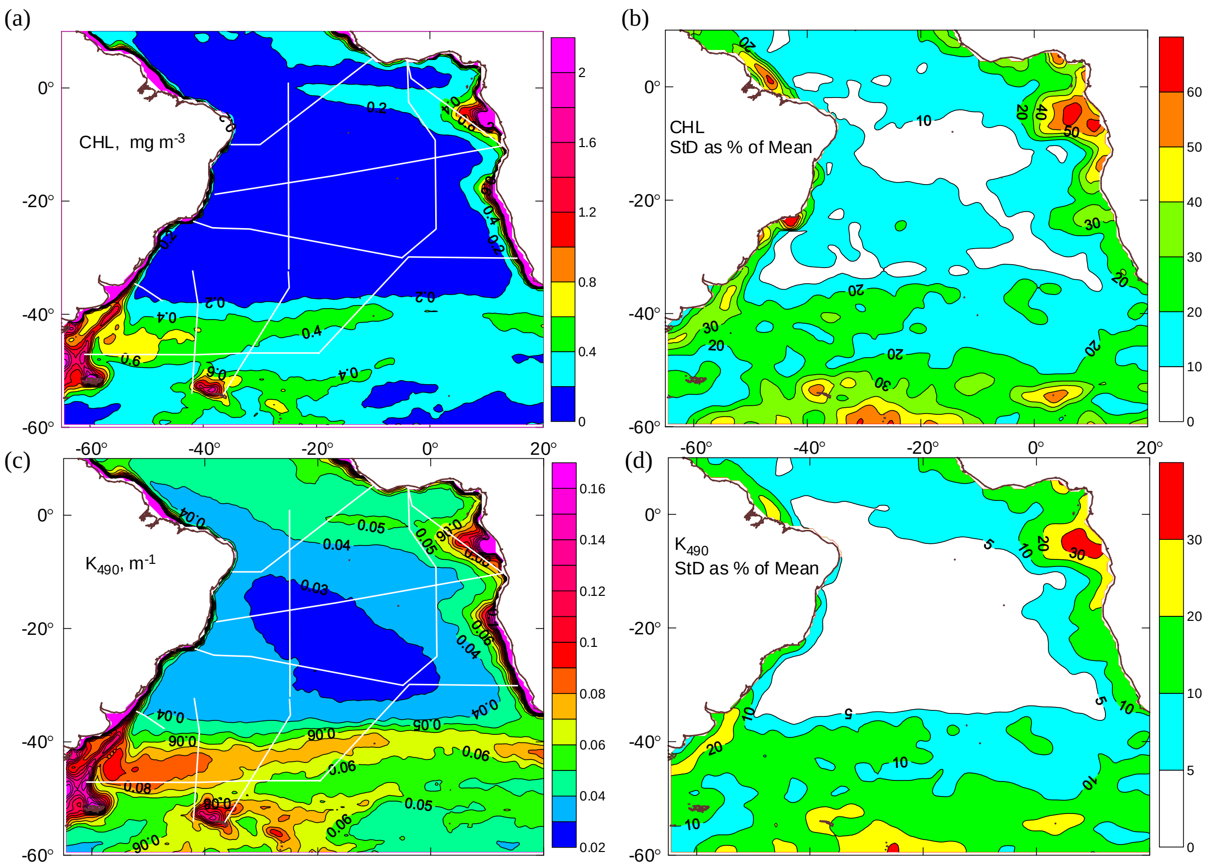

Fig. 2. SeaWiFS derived parameters and interannual variability: (a) Chlorophyll concentration (CHL)—five-year average. (b) Standard deviation of the CHL as percentage of five-year mean. (c) Diffuse attenuation coefficient (K_{490})—five-year average. (d) Standard deviation of the K_{490} as percentage of five-year mean.

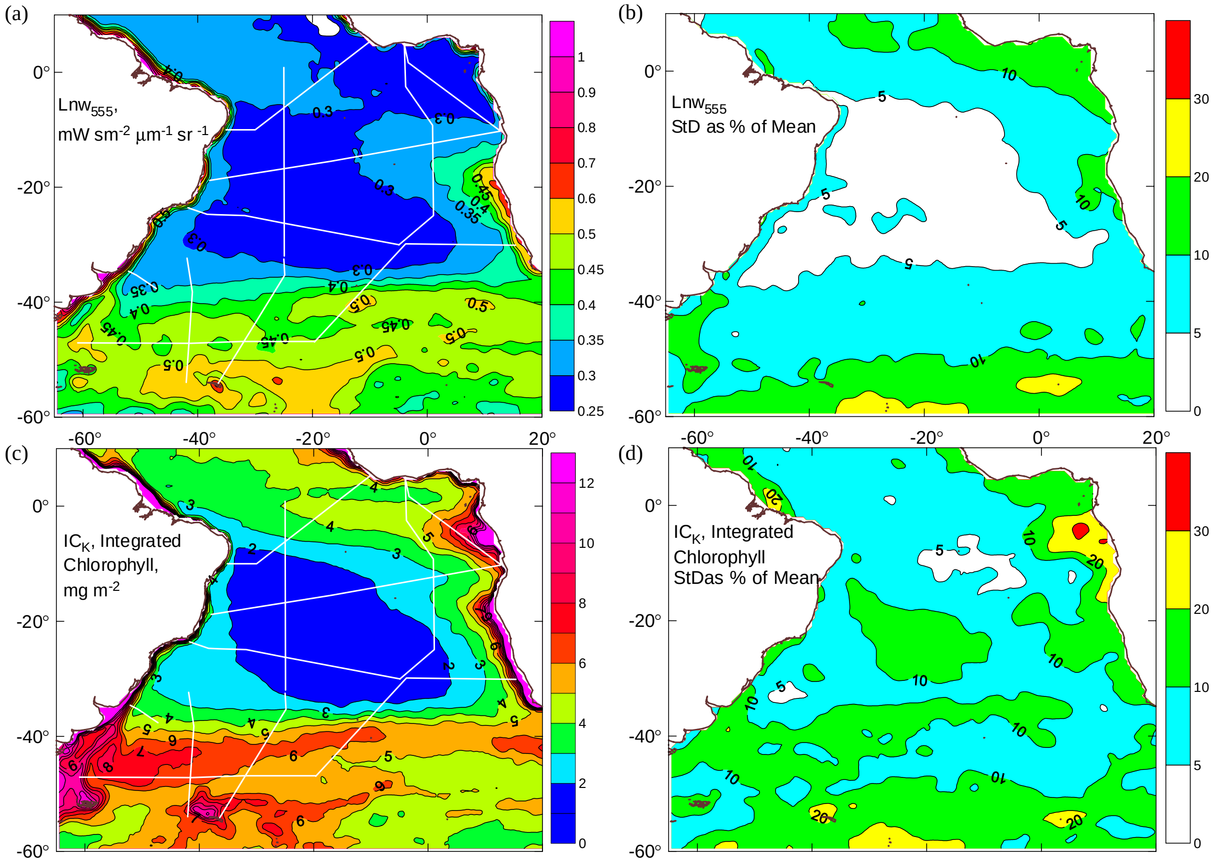

Fig. 3. SeaWiFS derived parameters and interannual variability: (a) Normalized water-leaving radiation at 555 nm wavelength $L_{WN}(555)$—five-year average. (b) Standard deviation of the $L\mathrm{nw}_{555}$ as percentage of five-year mean. (c) Integrated Chlorophyll concentration (IC_K)—five-year average. (d) Standard deviation of the IC_K as percentage of five-year mean.

Supplement1.htm. The numerical values of the parameters were extracted from the grid along the SAVE lines and were used for correlation analysis.

Data obtained from SAVE cruises during austral summers from 1987 to 1989 were pooled into a combined data set. We averaged beam attenuation data and calculated POC concentrations (using the regression shown in Fig. 4b) over one attenuation depth (z) for each profile. For determination of one attenuation depth we used: $z = 1/K_{490}$ (see Gordon and McCluney, 1975 where they called it "penetration depth") and made our estimate of z based on SeaWiFS-derived K_{490} averaged over 5 austral summers. The attenuation depth would be better determined by direct measurements, but this parameter was not measured during SAVE cruises. The equation used yielded very reasonable results. As can be seen in Fig. 4a, values of z varied from 35 m at the center of the South Atlantic gyre to 10 m near shore, and 2–5 m in the La Plata estuary and Congo River outflow, which are about what one might expect (Arst et al., 2002).

SAVE data were averaged over one attenuation depth, interpolated to a regular 0.5° grid, smoothed by averaging data within the nearest $1.5° \times 1.5°$ for each grid node, and values of c_p (Fig. 4c) and POC (Fig. 4d) were extracted from the grid along the cruise tracks. Such an approach allowed us to construct uniform, comparable, sea-collected and satellite-derived data sets where all data prepared for comparative analyses have exactly the same spatial location. This allowed us

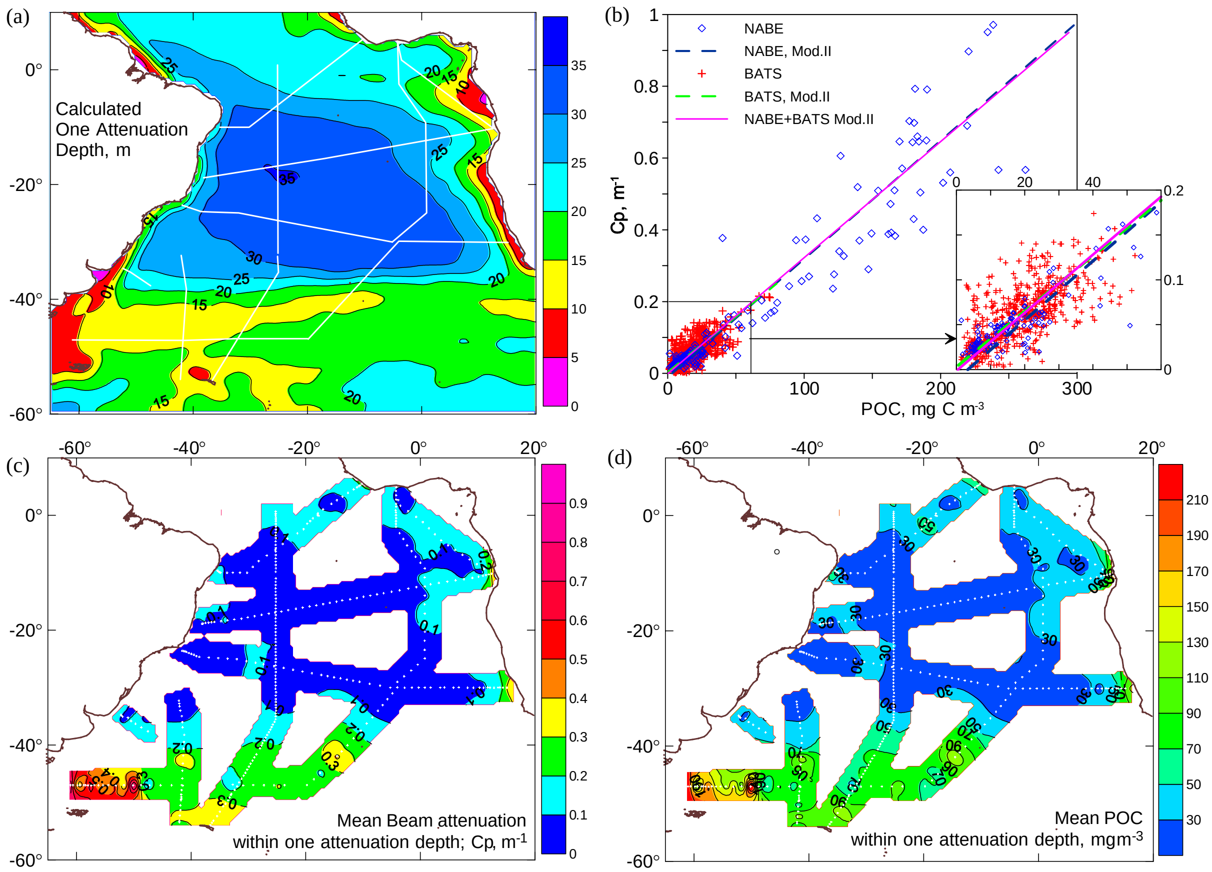

Fig. 4. (a) Spatial distribution of the one attenuation depth estimated from SeaWiFS-derived K_{490} (see text). (b) Model II regression between beam attenuation and POC concentration based on combined NABE and BATS data. (c) Mean beam attenuation due to particles down to one attenuation depth in the South Atlantic based on SAVE data. (d) Mean POC concentration down to one attenuation depth in the South Atlantic calculated from beam attenuation.

to develop a statistically sufficient data set with more than 850 generated data pairs along the cruise track lines during each austral summer season (1997–2002) for comparing beam attenuation, calculated POC and four SeaWiFS-derived variables ($L_{WN}(555)$, CHL, K_{490}, and IC_K).

3. Results and discussion

Data from different SAVE cruises were tested for interannual/intercruise variability. For that we overlay beam *c* profiles obtained during different cruises on stations that were located at crossings, i.e. in close proximity (within 0.5° longitude–latitude circle) to each other. A total of nine crossings were available (see boxes (i) to (ix) in Fig. 1).

Comparison of the deep-water part of the beam *c* profiles (∼250–∼4000 m) shows very good agreement for all crossings, therefore we include here only the upper 250 m layer for illustration (Fig. 5). For hydrographic relations the profiles of water density are also plotted. Temperature, salinity and beam attenuation values averaged over one attenuation depth are shown in Table 2. Values of SeaWiFS-derived Chl, K_{490} and $L_{WN}(555)$ averaged over austral summers from 1997–2002 for $72 \times 72\,\text{km}^2$ pixels spots obtained from the crossing areas are included in the table.

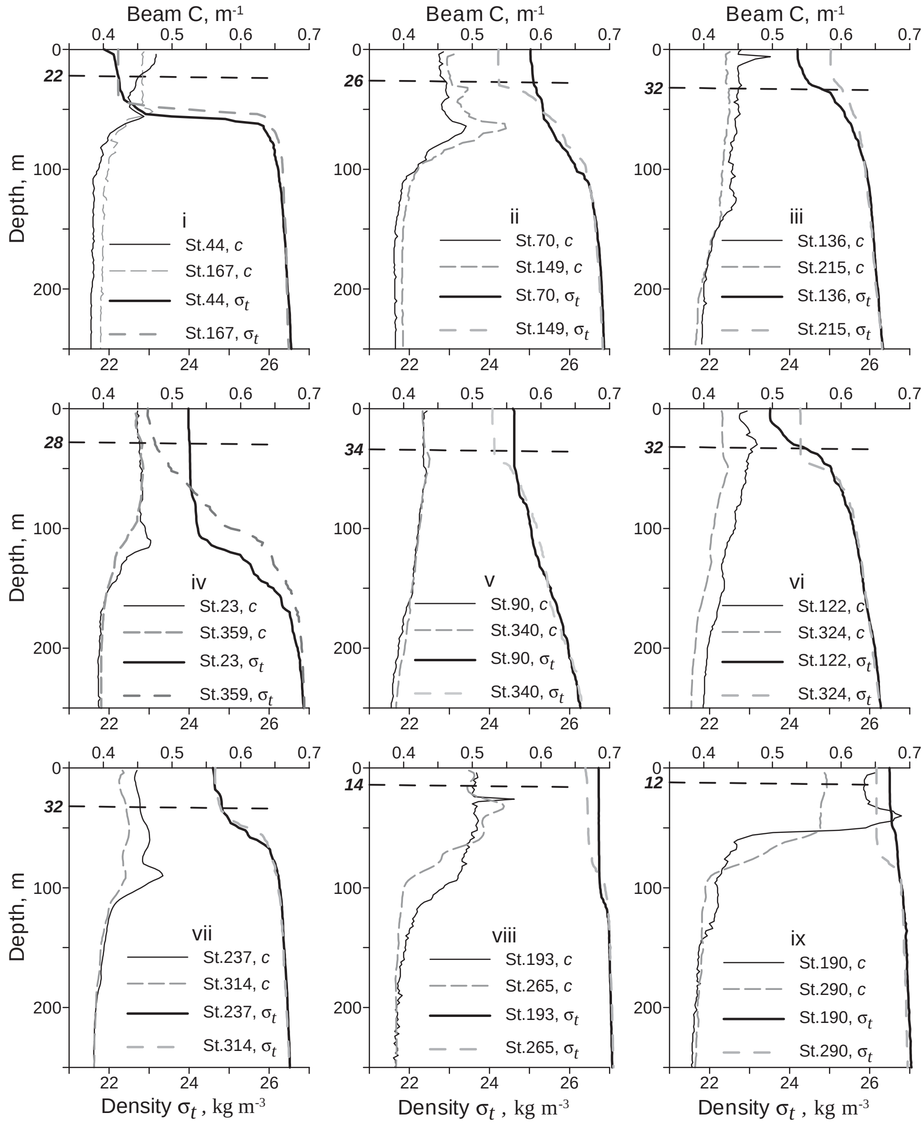

Fig. 5. Beam attenuation (upper *X*-axis) and density (lower *X*-axis) profiles from the SAVE stations located at the cruise crossing points (see Fig. 1). One attenuation depth (see Fig. 4a) denoted by dashed line. Station data shown in Table 2.

As can be seen from Fig. 5 and Table 2, measurements show very good agreement of the beam *c* values from different cruises along the profiles as well as averaged within one attenuation depth. Interannual differences would be expected for this dynamic portion of the upper water column, especially in the area with high concentrations (e.g., Patagonian shelf—crossing ix). The low interannual variability validated our first-order approach of combining SAVE field data acquired during austral summers 1987–1989 into one data set representing this season.

We note that diurnal variations in beam *c* occur in some regions of the ocean but not all (Siegel et al., 1989; Gardner et al., 1995, 1999, 2000, 2001; Kinkade et al., 1999). Without diurnal measurements at each site (which were not made) its influence cannot be determined. However, in each

Table 2
Data from SAVE stations at the cruises crossing points (see Fig. 1) averaged over one attenuation depth layer and SeaWiFS data for same locations averaged over austral summers from 1997 to 2002 for $72 \times 72\,km^2$ (8×8 pixels) areas

Crossing		SAVE data							SeaWiFS data			
#	St #	Lon.	Lat.	Date	Time	Beam C	Temp.	Salinity	Year	CHL	K_{490}	$L_{WN}(555)$
i	44	−3.59	3.00	19-Dec-87	22:12	0.467	28.702	34.965	97–98	0.182	0.044	0.268
	167	−3.92	2.50	05-Mar-88	1:05	0.457	29.179	35.293	98–99	0.127	0.038	0.247
									99–00	0.146	0.040	0.268
									00–01	0.171	0.044	0.288
									01–02	0.136	0.040	0.286
ii	70	−0.50	−12.59	04-Jan-88	5:30	0.455	22.961	36.465	97–98	0.093	0.036	0.321
	149	1.00	−12.33	25-Feb-88	0:05	0.466	25.757	36.476	98–99	0.122	0.039	0.342
									99–00	0.096	0.035	0.309
									00–01	0.110	0.037	0.333
									01–02	0.091	0.035	0.298
iii	136	−5.00	−30.00	15-Feb-88	11:33	0.457	23.579	35.791	97–98	0.041	0.029	0.275
	215	−3.77	−29.86	04-Jan-89	23:50	0.434	21.945	36.128	98–99	0.039	0.029	0.272
									99–00	0.042	0.029	0.285
									00–01	0.039	0.029	0.265
									01–02	0.043	0.030	0.286
iv	23	−25.00	−6.18	01-Dec-87	1:24	0.450	26.293	36.388	97–98	0.091	0.035	0.303
	359	−24.98	−6.00	05-Apr-89	3:04	0.451	28.598	36.122	98–99	0.085	0.034	0.290
									99–00	0.094	0.035	0.307
									00–01	0.092	0.035	0.288
									01–02	0.113	0.036	0.297
v	90	−25.00	−16.77	14-Jan-88	10:50	0.429	26.474	37.295	97–98	0.037	0.029	0.292
	340	−24.96	−16.50	29-Mar-89	18:41	0.429	27.858	37.199	98–99	0.032	0.029	0.287
									99–00	0.031	0.028	0.282
									00–01	0.032	0.028	0.284
									01–02	0.032	0.029	0.284
vi	122	−25.50	−26.16	07-Feb-88	20:35	0.464	27.203	36.509	97–98	0.070	0.033	0.311
	324	−24.94	−26.00	24-Mar-89	13:56	0.427	26.023	36.650	98–99	0.044	0.030	0.272
									99–00	0.055	0.031	0.305
									00–01	0.054	0.031	0.299
									01–02	0.044	0.030	0.277
vii	237	−25.00	−32.50	01-Feb-89	13:45	0.450	22.095	35.657	97–98	0.057	0.031	0.276
	314	−24.92	−31.97	21-Mar-89	6:09	0.428	22.115	35.650	98–99	0.057	0.031	0.283
									99–00	0.057	0.031	0.297
									00–01	0.056	0.031	0.284
									01–02	0.051	0.030	0.275
viii	193	−32.50	−46.86	22-Dec-88	9:20	0.504	6.193	33.994	97–98	0.230	0.050	0.411
	265	−31.50	−46.85	12-Feb-89	0:03	0.498	8.844	34.161	99–00	0.287	0.056	0.434
									00–01	0.399	0.067	0.453
									01–02	0.431	0.070	0.487
ix	190	−41.26	−47.16	18-Dec-88	18:57	0.638	12.104	34.487	97–98	0.344	0.064	0.455
	290	−41.55	−47.00	22-Feb-89	11:54	0.578	10.226	34.471	98–99	0.523	0.077	0.475
									99–00	0.483	0.076	0.425
									00–01	0.564	0.081	0.468
									01–02	0.483	0.076	0.449

region with similar satellite optical signal we have many stations and some were taken at night and others during the day. The processing and spatial averaging of the c_p sections also decreases the variation of the in situ data. Presumably some of the scatter in c_p with respect to satellite products is due to diurnal variation in beam c. Scatter in c_p/POC (see Fig. 4b) also could result from differences in particle size (Zaneveld, 1973) as the plankton community varies seasonally and regionally, but we have no data to make any adjustments.

Although we are focusing on the layer down to one attenuation depth (denoted by dashed lines in Fig. 5), in several locations the beam attenuation maximum is located below one attenuation depth (Fig. 5: crossing ii, iv, vii, viii and ix). One important inference is that a large amount of the optically reactive matter is not detected by remote sensing data. Thus integrated POC standing stock could be very different from what we are seeing within one attenuation depth. This is the same limitation dealt with in comparing ocean color products with in situ chlorophyll measurements. There is, however, very good agreement between the mean POC concentration down to one attenuation depth and remotely sensed data, as will be demonstrated.

Given that the years in which the SAVE and SeaWiFS data were collected did not overlap, it is important to establish the magnitude of interannual variability in seasonally averaged SeaWiFS data products. To assess interannual variation we have calculated seasonal five-year mean and standard deviation values for every grid node for four variables. In Figs. 2b,d and 3b,d the standard deviations of the all four parameters are presented as a percent of the seasonal five-year mean (Figs. 2a,c and 4a,c). Clearly, the deviation of the parameters K_{490} and $L_{WN}(555)$ is very low ($<5\%$) over the large area of the South Atlantic gyre. The maximum variation in the entire South Atlantic was 30% (for K_{490}, Fig. 2d); within the area affected by the Congo River outflow and at the southern portion of the region along the Sub-Antarctic front. The $L_{WN}(555)$ field showed even less interannual variation all around the region. It was only about 10% even in near-shore areas, exceeding 20% only in the southern margin, again, along the Sub-Antarctic front (Fig. 3b). Calculated values such as CHL and IC_K show higher deviations, which is quite understandable since these variables are more closely related to primary production than to the concentration of total biogenic material in surface waters. Nevertheless, their deviation is still reasonably low—most of the region shows 0–20% variation with maxima obviously connected to the maxima in the K_{490} field (since K_{490} is used for calculating both of these parameters). It is noteworthy that even highly productive areas around the Falkland Islands, the adjoining Patagonian shelf, Benguela upwelling zone, and Sub-Antarctic front are detected during all years showing low interannual variation, indicating that the fields of these features have almost the same order of magnitude intensity and spatial position in that particular season when averaged over the entire season. Generally speaking, the CHL, K_{490}, and IC_K exhibit greatest variation from year to year in their mid- to high-values, with variations decreasing at the very low end of their range (Figs. 2b,d and 3b,d). $L_{WN}(555)$ proved to have the least variation over the entire period of time. Similar results were reported recently by Doney et al. (2003) for daily level SeaWiFS ocean-color data (CHL).

There could be several reasons for differences in the variability of the K_{490} (and derived parameters). The most important may be the uncertainty in SeaWiFS imagery caused by errors in the atmospheric-correction bands, which are propagated and exaggerated to the visible bands and to the chlorophyll product through the atmospheric-correction process (Hu et al., 2001). This factor sometimes produced negative values of the normalized water leaving radiance at 412 and 443 nm, i.e. at SeaWiFS bands 1 and 2 (McClain et al., 2000). The geographical distribution of the negative normalized water-leaving radiance shows the largest problems to be in the coastal margins. It is even more interesting to find that the Congo River outflow area is a region where the negative values occur most of the time (Figs. 6 and 9 in McClain et al., 2000). Taking into account that these values have been used in the both OC2v4 (Ocean chlorophyll algorithm 2, ver. 4; O'Reilly et al., 1998), and OC4 (Ocean Chlorophyll Algorithm 4), as well as in calculation of K_{490} (O'Reilly et al., 2000), it is not surprising that a great deal of variability was detected for these three parameters (K_{490}, Chl, IC_K) near the Congo River outflow. This could be one reason why normalized water leaving radiance at 555 nm showed the lowest variation over the five-year span. As a result of this assessment, we suggest that using the "different year–same season" approach for data analysis and comparison is reasonable when using seasonally averaged $L_{WN}(555)$. Use of the other SeaWiFS products we tested may be satisfactory in areas not affected by the above mentioned influences.

The plan view map of the spatial distribution of measured beam attenuation and calculated POC integrated over one attenuation depth are shown in Figs. 4c and d. Realizing that the years in which the SAVE and SeaWiFS data were collected did not overlap, and considering the large difference in the spatial and temporal scales of coverage, it is highly encouraging that there is such good general agreement in the distribution and intensity of c_p-derived POC and the four SeaWiFS parameters (see Figs. 2a,c, 3a,c and 4d).

A comparison of POC and SeaWiFS products for each year, as well as for five-year averages along all SAVE tracks (shown as white lines in Figs. 2a,c and 3a,c) demonstrates that most of the maxima in SeaWiFS products match the location of the elevated POC values very well. High values are observed in upwelling areas off southern Africa, near the Congo River outflow, in the central equatorial region, near the shelf off southern South America and in the Argentine Basin where eddy-kinetic energy is high and may be pumping nutrients into surface waters (Richardson et al., 1993). However, the patterns of normalized water-leaving radiation at 555 nm appear to be the best match. The major area of disagreement of the other three SeaWiFS products is along transect 2a and east of transect 2b (Fig. 1), where they show a major maxima that is not seen in either the c_p/POC or in any of the years of $L_{WN}(555)$ data. The possible reasons for that will be discussed below.

Creating property–property diagrams and calculating a correlation coefficient is a more quantitative method of determining which SeaWiFS product best fits the POC data (see Fig. 6). A log-function proved to be the best fit for the data. We also applied a Model II linear regression, which demonstrated a slightly lower, but still reasonable correlation (Table 3). Analyzing Fig. 6 it is clear that for K_{490} and related parameters (CHL, IC_K) the general distributions of data contain at least one sub-set of data that does not follow the general trend. High K_{490} (or CHL or IC_K) values and low $L_{WN}(555)$ and calculated POC values characterize these data (diamonds in Fig. 6). The most likely reason for this deviation is that these data were obtained in an areas that included either Case II waters with terrigenous input from river outflow or waters where colored dissolved organic matter (CDOM) absorption generally exceeded phytoplankton pigment absorption at 443 nm. It is well known that the SeaWiFS chlorophyll algorithms often produce unreliable results in such situations (Burenkov et al., 2000; Del Castillo et al., 2001; Toole and Siegel, 2001; Murphy et al., 2001; Barlow et al., 2001; Desa et al., 2001; Thomas et al., 2001; Clementson et al., 2002). In our initial analysis of these data sets we used Reprocessing Version 3 of SeaWiFS data (not shown), but we repeated all calculations and maps using Reprocessing Version 4 data when they became available. Comparing results from the two reprocessing versions it is clear that Version 4 gives better results; however, in complicated coastal environments further refinement is still necessary.

Analysis of the spatial distribution of the data shows that the outlying values are indeed from areas likely to be affected by the Congo River discharge or from stations located close to the coast or islands (see Section 2a denoted by the gray shadow in Fig. 1 and black diamonds data points in Fig. 6a,b and d). It is likely that values of K_{490}, CHL, and IC_K in these particular locations are unreliable. In addition, it should be noted that most of the optical signal in those areas comes from the upper 5–10 m of water (one attenuation depth—see Fig. 4a) and maxima of the POC

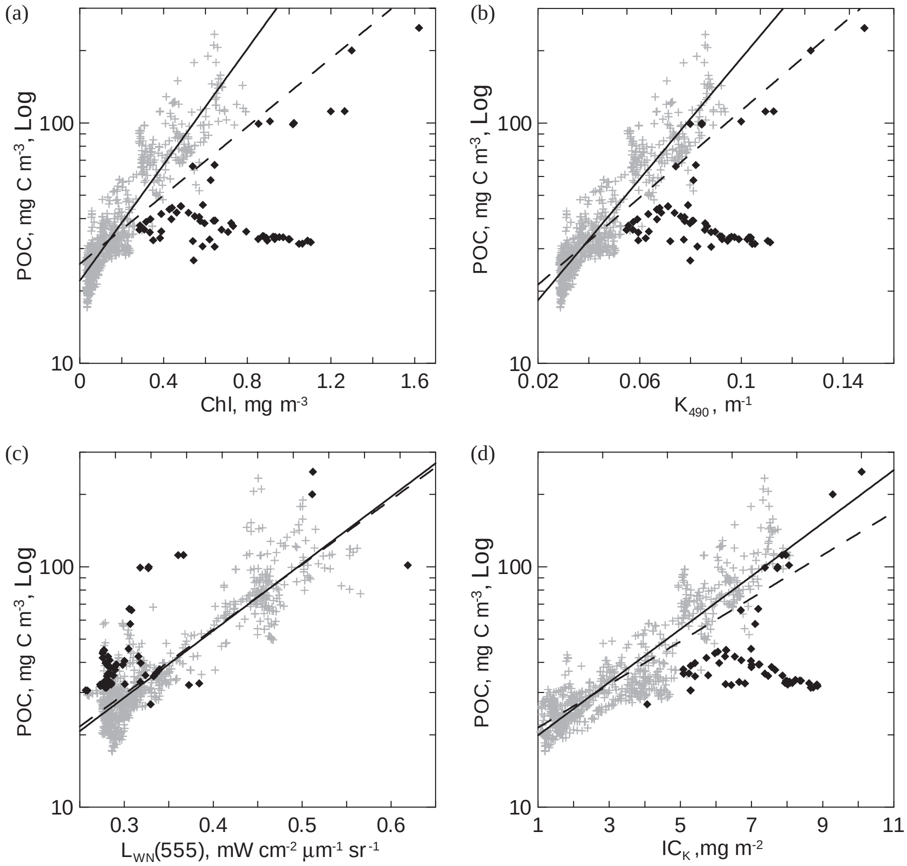

Fig. 6. Calculated POC (from beam c_p) vs. SeaWiFS derived products averaged over five years for austral summers (December–April) from 1997 to 2002 along SAVE lines. (+)—Data from open ocean area. (◇)—Data from coastal area (denoted in Fig. 1 by gray shadow). Dashed line—exponential regression based on all data. Solid line—exponential regression based on open ocean data only. (a) CHL-Chlorophyll-*a* concentration, mg m^{-3}; (b) K_{490}—Diffuse attenuation coefficient at 490 nm wavelength, m^{-1}; (c) $L_{WN}(555)$—Normalized water-leaving radiance at 555 nm wavelength, mW cm^{-2} µm^{-1} sr^{-1}; (d) IC_K -Integrated Chlorophyll-*a* concentration, mg m^{-2}.

concentration are located below one attenuation depth. A similar situation has been observed recently in the vicinity of the Zambezi plume (Siddorn et al., 2001). We removed these data from the analysis, and, not surprisingly, correlations between c_p and K_{490}, CHL, and IC_K improved significantly, while for $L_{WN}(555)$ it improved only slightly. Data from the Congo River region did not appear so anomalous in the $L_{WN}(555)$ data, so removal of those data did not change its correlation with POC. Statistical data for the regressions in Fig. 6 are provided in Table 4 with and without the outlier data.

When using all data, the best correlation between c_p/POC and the four products investigated was with $L_{WN}(555)$ (Fig. 6c). For each year in consideration the regression was quite similar and the correlation coefficients for different years were between 0.79 and 0.82 (Model II, see Table 3). A logarithmic fit of the data produced $r = 0.88$ when using satellite data averaged over five years (Table 4). The relation observed between POC and CHL concentration derived from SeaWiFS data was considerably weaker with r varying from 0.43 to 0.83 for different years (see Table 3). A similar situation exists with K_{490} having a comparable r:

Table 3
Parameters of linear regression (Model II) between POC calculated from SAVE beam attenuation coefficient data (averaged over one attenuation depth) and different SeaWiFS derived products (Reprocessing 4) acquired during 1997–2002, both averaged over austral summer (December–April) for South Atlantic area

Parameters of the regression	Austral summers (December–April), Model II regression, $n = 854$				
	1997–1998	1998–1999	1999–2000	2000–2001	2001–2002
POC vs. *CHL*					
Slope	8.394×10^{-3}	7.754×10^{-3}	8.690×10^{-3}	7.366×10^{-3}	8.081×10^{-3}
Intercept	−0.161	−0.116	−0.153	−0.102	−0.127
Slope SD	2.597×10^{-4}	1.477×10^{-4}	2.454×10^{-4}	1.621×10^{-4}	1.889×10^{-4}
Intercept SD	1.502×10^{-2}	0.815×10^{-2}	1.394×10^{-2}	0.900×10^{-2}	1.053×10^{-2}
R	0.428	0.831	0.565	0.766	0.730
POC vs. K_{490}					
Slope	6.809×10^{-4}	6.849×10^{-4}	7.019×10^{-4}	6.478×10^{-4}	6.94×10^{-4}
Intercept	1.529×10^{-2}	1.704×10^{-2}	1.650×10^{-2}	1.866×10^{-2}	1.697×10^{-2}
Slope SD	1.979×10^{-5}	1.275×10^{-5}	1.812×10^{-5}	1.351×10^{-5}	1.538×10^{-5}
Intercept SD	1.129×10^{-3}	7.029×10^{-4}	1.018×10^{-3}	7.482×10^{-4}	8.545×10^{-4}
R	0.528	0.839	0.656	0.793	0.762
POC vs. $L_{WN}(555)$					
Slope	2.597×10^{-3}	2.677×10^{-3}	2.244×10^{-3}	2.366×10^{-3}	2.550×10^{-3}
Intercept	0.228	0.223	0.240	0.231	0.221
Slope SD	5.459×10^{-5}	5.206×10^{-5}	4.686×10^{-5}	4.671×10^{-5}	5.178×10^{-5}
Intercept SD	3.026×10^{-3}	2.875×10^{-3}	2.596×10^{-3}	2.581×10^{-3}	2.864×10^{-3}
R	0.786	0.823	0.792	0.817	0.805
POC vs. IC_K					
Slope	6.735×10^{-2}	7.032×10^{-2}	7.009×10^{-2}	6.784×10^{-2}	7.081×10^{-2}
Intercept	0.677	0.622	0.661	0.749	0.609
Slope SD	1.829×10^{-3}	1.455×10^{-3}	1.761×10^{-3}	1.496×10^{-3}	1.615×10^{-3}
Intercept SD	0.103	0.801	0.099	0.083	0.090
R	0.609	0.796	0.677	0.764	0.745

varying from 0.53 in 1997–1998 to 0.84 in 1998–1999. Integrated Chlorophyll (IC_K) shows a correlation close to its "parents" (CHL and K_{490}), with r between 0.61 and 0.80. In all cases the logarithmic fit between POC and SeaWiFS products produced a better statistical correlation than a linear Model II regression (Tables 3 and 4).

When the coastal data were removed and correlations were obtained for "open ocean" data, the correlation coefficients were very similar for all parameters (Table 4). For example, the correlation coefficients for the exponential fit with POC ranged between 0.91 and 0.93. In this paper, we favor the use of the POC/$L_{WN}(555)$ relationship because it is more likely to yield the same results whether or not Case II waters are encountered. That is, as can be graphically seen in Fig. 6c, the exponential fit for data with and without Case II waters is virtually identical. Although the POC/$L_{WN}(555)$ relationship shown in Fig. 6c has a reasonable regression coefficient, we propose it only as a first-order algorithm because the shipboard and satellite data were not concurrent. Clearly, it is important to collect synchronous data in the future in different bio-optical provinces.

A direct comparison of our algorithms with those of Stramski et al. (1999) is desirable, but not possible with these data because we were working in very different areas—the South Atlantic vs. the Ross Sea/Southern Ocean sector of the Pacific. The slopes of the empirical regressions of Stramski et al. (1999) for POC vs. particle backscattering

Table 4
Regressions between c_p, calculated POC (both averaged over one attenuation depth) and different SeaWiFS products (Reprocessing 4 version) averaged over 5 years (1997–2002), for austral summer (December–April)

Parameters of the regressions	SeaWiFS (Rep.4) ocean color products, 5-years mean							
	CHL		K_{490}		$L_{WN}(555)$		IC_K	
	All data	Open ocean	All data	Open ocean	All data	Open ocean	All data	Open ocean
SeaWiFS vs. cp								
Model II: c_p = Slope × SeaWiFS + Intercept								
Slope	0.428	0.514	4.989	5.702	1.348	1.370	0.048	0.053
Intercept	0.044	0.041	−0.095	−0.114	−0.316	−0.325	−0.038	−0.043
Slope SD	0.010	0.009	0.113	0.093	0.026	0.027	0.001	0.001
Intercept SD	0.004	0.002	0.006	0.005	0.009	0.009	0.005	0.004
R	0.705	0.879	0.750	0.888	0.825	0.829	0.735	0.837
Exponential fit: $c_p = e^{\text{power}\times\text{SeaWiFS}} \times$factor								
power	1.659	2.451	21.080	27.827	6.274	6.464	0.209	0.256
Factor	0.082	0.074	0.044	0.034	0.014	0.013	0.055	0.049
RMS	0.132	0.063	0.104	0.045	0.065	0.062	0.093	0.050
R	0.734	0.890	0.800	0.923	0.880	0.892	0.821	0.913
SeaWiFS vs POC								
Model II: POC = Slope × SeaWiFS + Intercept								
Slope	131.6	158.3	1532.0	1754.5	414.9	421.7	14.8	16.301
Intercept	14.304	13.259	−28.453	−34.395	−69.369	−99.336	−10.960	−12.608
Slope SD	3.183	2.649	34.565	28.236	7.946	8.243	0.342	0.312
Intercept SD	1.096	0.766	1.807	1.382	2.770	2.895	1.496	1.277
R	0.707	0.881	0.753	0.890	0.823	0.833	0.738	0.840
Exponential Fit: POC = $e^{\text{power}\times\text{SeaWiFS}} \times$factor								
Power	1.641	2.395	20.848	27.534	6.209	6.397	0.207	0.253
Factor	25.918	23.410	14.017	10.867	4.586	4.237	17.414	15.475
RMS	0.129	0.061	0.640	0.043	0.062	0.060	0.091	0.049
R	0.735	0.891	0.800	0.924	0.882	0.893	0.822	0.914

Regressions based on all data ($n = 854$) and *open ocean* data only ($n = 783$) are given.

coefficient b_{bp} at 510 nm for the Ross Sea and Antarctic Polar Front Zone differed by more than a factor of 28, so clearly there is a potential for regional differences. However, differences in their correlation between backscatter and R_{rs} were much smaller. They chose to use the Polar Front algorithm for further processing. We do not yet know the regional variability of our algorithm. The SeaWiFS data available for comparison with ship-board data had sun-lighting conditions with the sun zenith angle being between 58° and 73°, which is not optimal. Also, the ship (*NB Palmer*) was located within a single small area of the visible open water at the edge of a massive cloud field. They used the best data available, and it will be important to compare our two approaches when simultaneous optical, POC and ocean-color data are collected simultaneously in the same region with clear skies and optimal lighting conditions.

The in-water optical measurements made by Stramski et al. (1999) were not made during the SAVE program, so their technique cannot be applied to data in the South Atlantic. However, we have data for the area studied by Stramski et al. (1999) with which we can make similar analyses as done for the South Atlantic, so this will allow us to compare methods more directly in the future. This also will allow us to quantify the magnitude of regional differences in our algorithms.

The in-water optical measurements made by Stramski et al. (1999) were not made during the SAVE program, so their technique cannot be applied to data in the South Atlantic. However, we have data for the area studied by Stramski et al. (1999) with which we can make similar analyses as done for the South Atlantic, so this will allow us to compare methods more directly in the future. This also will allow us to quantify the magnitude of regional differences in our algorithms.

To demonstrate the utility of an algorithm for estimating POC distribution on a basin-wide scale, it is a useful exercise to apply our regression to a recent seasonally or monthly averaged map of the North and South Atlantic for $L_{WN}(555)$. Thus we have constructed a map of POC distribution (Fig. 7a) based on $L_{WN}(555)$ SeaWiFS data for January 2001 using the POC$-L_{WN}(555)$ regression constructed on data averaged for five years:

$$\mathrm{POC} = 4.586e^{6.209\,L_{WN}(555)}, \quad r = 0.882.$$

From this map (Fig. 7a) it is clear that during austral summer most of the POC spatial variability is located in the South Atlantic with expected maxima in (1) upwelling zones off of Namibia and Angola (Benguela upwelling), (2) over the shelf areas (especially the Patagonian shelf and Amazon River outflow), and (3) in the Southern ocean (Sub-Antarctic Front). This application demonstrates the potential of the approach for calculating POC distributions from ocean-color products in addition to the traditional ocean-color pigment maps. We also note (though not illustrated here) that Reprocessing 4 version of SeaWiFS data yields significantly better results in near-shore areas compared to the previous Reprocessing 3 Version.

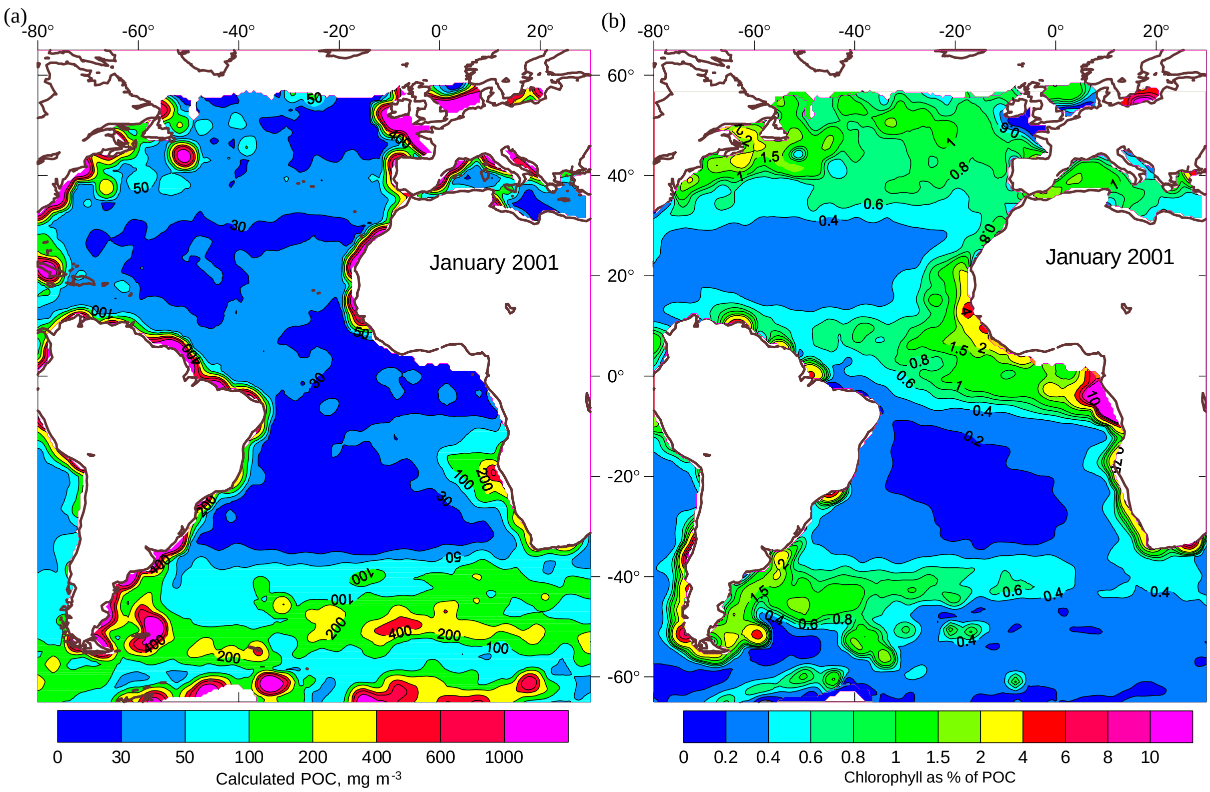

Fig. 7. (a) POC concentration down to one attenuation depth in the Atlantic Ocean calculated from SeaWiFS-derived $L_{WN}(555)$ data for January 2001 and (b) chlorophyll as a percentage of POC (see text).

It is well known that models of carbon fixation rely on chlorophyll concentration data, and such models are continually improving (Taylor et al., 1992; Behrenfeld and Falkowski, 1997). However, when it comes to predicting total carbon abundance one needs more than just chlorophyll abundance because the bulk carbon to chlorophyll ratio ranges broadly (Chung et al., 1996).

To illustrate this relationship more clearly it is more intuitive to display the inverse of the carbon to chlorophyll ratio, because this provides chlorophyll as a percentage of the carbon present. Using our basin-wide map of POC concentration we can roughly calculate chlorophyll as a percentage of particulate carbon using the SeaWiFS chlorophyll average for the same month for which we mapped POC (January 2001). This map (Fig. 7b) shows that chlorophyll is only 0.2% to about 2% of the POC concentration in surface waters of the open ocean. This makes it easier to realize that while most POC in the open ocean is associated with chlorophyll, there is an order of magnitude range in the POC:Chl ratio, Therefore one should not expect chlorophyll to be a very quantitative proxy for carbon because it represents only a small percentage of organic matter in the ocean. Furthermore, that percentage changes vertically and temporally as primary productivity varies and organisms are consumed or decompose. The percentage chlorophyll map (Fig. 7b) highlights the oligotrophic nature of the central gyres in the central north and south Atlantic. It also demonstrates that in this particular season, chlorophyll is relatively more abundant north of 30°N in the Atlantic, in the north equatorial region, and along 40°S.

Note that the areas of greatest POC concentrations in the Southern Ocean (shown as red in Fig. 7a) are not all correspondingly high in their percentage of chlorophyll (Fig. 7b). The area of highest percentage of chlorophyll in the South Atlantic is along the subtropical convergence zone at 40°S, a region of large POC gradients. The bands of elevated POC values along 50°S and 60°S are matched with elevated values of chlorophyll, so no increase in % chlorophyll appears. These differences may indicate the areas where primary production is active vs. areas where older, low-chlorophyll POC is accumulating.

The upwelling area off of Namibia and Angola shows high values of POC, but no real rise in % chlorophyll. The area of highest chlorophyll percentages (off the Congo River) does not have correspondingly high values of POC. As noted earlier, the area off the Congo River has been shown to have negative values in water-leaving irradiance (Figs. 6 and 9 in McClain et al., 2000). Thus, the high values of chlorophyll in this area are questionable, perhaps caused by false color readings because of the presence of DOM from outflow of the Congo.

4. Conclusions

The beam attenuation coefficient data can be used successfully and effectively for basin-wide investigation of the spatial and temporal variability of particulate matter distribution, including POC. The good correlation of the ship-derived optical properties with satellite derived data averaged over comparable seasons (even though obtained in different years) is encouraging. This provides confidence in the use of "same season–different year" comparisons of satellite information with historical data sets of light transmission on ocean basin scales when coincident data are not available, at least when averaged on seasonal time scales. A maximum interannual variability of 20–30% in the calculated concentration of POC is within reasonable limits for estimates of oceanographic parameters on a basin-wide scale. Variability in most of the area studied was $<10\%$.

Our analysis indicates that, of the SeaWiFS products we tested, $L_{WN}(555)$ is the most reliable parameter to serve as a proxy of POC assessed over a wide range of water conditions and shows high interannual reproducibility when seasonally averaged. It is not affected by the anomalous signal generated by waters from river outflow and/or coastal waters. Furthermore, this SeaWiFS product does not require additional data preprocessing or data filtration in order to produce a meaningful approximation of POC concentration. Using this parameter it was possible to assess the basin-wide distribution of the POC based on satellite data with acceptable accuracy. We expect that when comparisons are made for seasons when ship data and satellite data are collected synchronously, the correlation will be even better.

SeaWiFS data on $L_{WN}(555)$, CHL and K_{490} has been greatly improved after Reprocessing 4, especially in coastal areas but some uncertainties still exist near the river outflow zone and close to the coast. However, it also should be noted that in Case I waters the differences between satellite products we tested as proxies of POC might be less noticeable. We will test this issue in our future analysis using simultaneously collected field and satellite data.

While the intent of this paper was to demonstrate the ability to predict POC concentration in surface waters, our analysis also shows that a significant portion of the POC standing stock is located below one attenuation depth, which is also an issue with chlorophyll distribution. We will quantify this issue in future work.

Acknowledgements

This work was performed under the grant "Global Synthesis of POC Using Satellite Data Calibrated with Transmissometer and POC Data from JGOFS/WOCE", funded by NSF, grant #OCE9986762. We thank the graduate students (Brett Berglund and Megan Wood), technicians and scientists from the SAVE program who assisted in our participation in these cruises. Help from personnel at the SIO Ocean Data Facility (especially Mary Johnson, Bob Williams, Carl Mattson, and Dr. Jim Swift) were particularly valuable. We are grateful to four anonymous reviewers for very useful remarks and suggestions and to Dr. V.I. Haltrin from US NRL Code 7333—Ocean Optics for valuable advice. This is US JGOFS Contribution No. 850.

References

Afonin, E.I., Mishonov, A.V., Yunev, O.A, Williams, R., 1999. Bio-optical investigation of the Amazon outflow region in different seasons. In: IUGG XXII General Assembly, Birmingham, UK 1999. Abstracts Vol. B, p. B.242 (P15/W/03-B3).

Arst, H., Haltrin, V.I., Arnone, R.A., 2002. Informative water layer determined by attenuation depth, in water bodies of different turbidity. OCEANS 2002 MTS-IEEE Proceedings, Vol. 4. IEEE Catalog #: 02CH37362C, ISBN: 0-7803-7535-1.

Baith, K.S., Lindsay, R., Fu, G., McClain, C.R., 2001. SeaDAS: a data analysis system for ocean color satellite sensors. EOS, Transaction on AGU 82, 202.

Barlow, R.G., Aiken, J., Sessions, H.E., Lavender, S., Mantel, J., 2001. Phytoplankton pigment, absorption and ocean colour characteristics in the southern Benguela ecosystem. South African Journal of Science 97 (5–6), 230–238.

Bartz, R., Pak, H., Zaneveld, R.V., 1978. A transmissometer for profiling and moored observations in water. Proceedings of the society of photo-optical instrumentation engineers. Ocean Optics 160, 102–108.

Behrenfeld, M.J., Falkowski, P.G., 1997. Photosynthetic rates derived from satellite-based chlorophyll concentration. Limnology and Oceanography 42 (1), 1–20.

Berglund, B.L., 1989. The distribution of particulate matter in the equatorial and subtropical South Atlantic Ocean: Evidence for sources, transport and sinks of particles. MSc. in Oceanography Thesis. Department of Oceanography, Texas A&M University, December 1989. 95 pp.

Bishop, J.K.B., 1999. Transmissometer measurement of POC. Deep-Sea Research I 46 (2), 353–369.

Bishop, J.K.B., Calvert, S.E., Soon, M.Y.S., 1999. Spatial and temporal variability of POC in the northeast Subarctic Pacific. Deep-Sea Research II 46 (11–12), 2699–2733.

Burenkov, V.I., Kopelevich, O.V., Sheberstov, S.V., Vedernikov, V.I., 2000. Sea-truth measurements of the ocean color: validation of the SeaWiFS satellite scanner data. Oceanology 40 (3), 329–334.

Campbell, J.W., Blaisdell, J.M., Darzi, M., 1995. Level-3 SeaWiFS data Products: spatial and temporal binning algorithms. SeaWiFS Technical Report Series 32, 73.

Chung, S.P., Gardner, W.D., Richardson, M.J., Walsh, I.D., Landry, M.R., 1996. Beam attenuation and microorganisms: spatial and temporal variations in small particles along 140°W during 1992 JGOFS-EqPac transects. Deep-Sea Research II 43, 1205–1226.

Chung, S.P., Gardner, W.D., Landry, M.R., Richardson, M.J., Walsh, I.D., 1998. Beam attenuation by microorganisms and detrital particles in the equatorial Pacific. Journal of Geophysical Research-Oceans 103, 12669–12681.

Claustre, H., Morel, A., Babin, M., Cailliau, C., Marie, D., Marty, J-C., Tailliez, D., Vaulot, D., 1999. Variability in particle attenuation and chlorophyll fluorescence in the Tropical Pacific: scales, patterns, and biogeochemical implications. Journal of Geophysical Research-Oceans 104 (C2), 3401–3422.

Clementson, L.A., Parslow, J.S., Turnbull, A.R., McKenzie, D.C., Rathbone, C.E., 2002. Optical properties of waters in the Australasian sector of the Southern Ocean. Journal of Geophysical Research-Oceans 106 (C12), 31611–31625.

Del Castillo, C.E., Coble, P.G., Conmy, R.N., Muller-Karger, F.E., Vanderbloemen, L., Vargo, G.A., 2001. Multispectral in situ measurements of organic matter and chlorophyll fluorescence in seawater: documenting the intrusion of the Mississippi River plume in the West Florida shelf. Limnology and Oceanography 46 (7), 1836–1843.

Desa, E., Suresh, T., Matondkar, S.G.P., 2001. Sea truth validation of SeaWiFS Ocean colour sensor in the coastal waters of the Eastern Arabian Sea. Current Science 80 (7), 854–860.

Doney, S.C., Glover, D.M., McCue, S.J., Fuentes, M., 2003. Mesoscale variability of Sea-viewing Wide Field-of-view Sensor (SeaWiFS) satellite ocean color: global patterns and spatial scales. Journal of Geophysical Research-Oceans 108 (C2), 3024 (doi:10.1029/2001JC000843).

Dunne, J.P., Murray, J.W., Young, J., Balistrieri, L.S., Bishop, J., 1997. ^{234}Th and particle cycling in the central Equatorial Pacific. Deep-Sea Research II 44, 2049–2083.

Gardner, W.D., Biscaye, P.E., Zaneveld, J.R.V., Richardson, M.J., 1985. Calibration and comparison of the LDGO nephelometer and the OSU transmissometer on the Nova Scotian rise. Marine Geology 66, 323–344.

Gardner, W.D., Richardson, M.J., Walsh, I.D., Berglund, B.L., 1990. In-situ optical sensing of particles for determination of oceanic processes: what satellites can't see, but transmissometers can. Oceanography 3, 11–17.

Gardner, W.D., Walsh, I.D., Richardson, M.J., 1993. Biophysical forcing of particle production and distribution during a spring bloom in the North Atlantic. Deep-Sea Research 40, 171–195.

Gardner, W.D., Chung, S.P., Richardson, M.J., Walsh, I.D., 1995. The oceanic mixed-layer pump. Deep-Sea Research II 42, 757–775.

Gardner, W.D., Gundersen, J.S., Richardson, M.J., Walsh, I.D., 1999. The role of diel variations in mixed-layer depth on the distribution, variation, and export of carbon and chlorophyll in the Arabian Sea. Deep-Sea Research II 46, 1833–1858.

Gardner, W.D., Richardson, M.J., Smith, W.O., 2000. Seasonal patterns of water column particulate organic carbon and fluxes in the Ross Sea, Antarctica. Deep-Sea Research II 47, 3423–3449.

Gardner, W.D., Blakey, J.C., Walsh, I.D., Richardson, M.J., Pegau, S., Zaneveld, J.R.V., Roesler, C., Gregg, M.C., MacKinnon, J.A., Sosik, H.M., Williams III, A.J., 2001. Optics, particles, stratification and storms on the New England continental shelf. Journal of Geophysical Research 106, 9473–9497.

Gardner, W.D, Richardson, M.J., Carlson, C.A., Hansell, D., Mishonov, A.V., 2003a. Determining true particulate organic carbon: bottles, pumps and methodologies. Deep-Sea Research II 50 (3–4), 655–674.

Gardner, W.D., Mishonov, A.V., Richardson, M.J., 2003b. Global POC Distribution Assessed by Synthesis of JGOFS, WOCE and SAVE Transmissometer Data. In revision for Deep-Sea Research II.

Gordon, H.R., McCluney, W.R., 1975. Estimation of the depth of sunlight penetration in the sea for remote sensing. Applied Optics 14 (2), 413–416.

Gundersen, J.S., Gardner, W.D., Richardson, M.J., Walsh, I.D., 1998. Effects of monsoons on the seasonal and spatial distribution of POC and chlorophyll in the Arabian Sea. Deep-Sea Research II 45, 2103–2132.

Hu, C.M., Carder, K.L., Muller-Karger, F.E., 2001. How precise are SeaWiFS ocean color estimates? Implications of digitization-noise errors. Remote Sensing of Environment 76 (2), 239–249.

Kinkade, C.S., Marra, J., Dickey, T.D., Langdon, C., Sigurdson, D.E., Weller, R., 1999. Diel bio-optical variability observed from moored sensors in the Arabian Sea. Deep-Sea Research II 46, 1813–1831.

McClain, C.R., Barnes, R.A., Eplee, Jr., R.E., Franz, B.A., Hsu, N.C., Patt, F.S., Pietras, C.M., Robinson, W.D., Schieber, B.D., Schmidt, G.M., Wang, M., Bailey, S.W., Werdell, P.J., 2000. SeaWiFS Postlaunch Calibration and Validation Analyses, Part 2. In: Hooker, S.B., Firestone, E.R. (Eds.), NASA Technical Memorandum 2000-206892, Vol. 10, NASA Goddard Space Flight Center, 57pp.

Mishonov, A.V., Gardner, W.D., Richardson, M.J., 2000. Prospects for using historical transmissometer data in large-scale assessment of POC. In: 2000 Ocean Science Meeting, Jan. 2000, San Antonio, Texas. Supplement to EOS, Transaction, American Geophysical Union. December 1999. Abstracts, Vol. 80(49), p.122.

Morrison, J., Gaurin, S., Codispoti, L.A., Takahashi, T., Millero, F.J., Gardner, W.D., Richardson, M.J., 2001. Seasonal evolution of the hydrographic properties during the Antarctic Circumpolar current at 170°W during 1997–1998. Deep-Sea Research II 48, 3943–3972.

Murphy, R.J., Pinkerton, M.H., Richardson, K.M., Bradford-Grieve, J.M., Boyd, P.W., 2001. Phytoplankton distributions around New Zealand derived from SeaWiFS remotely sensed ocean colour data. New Zealand Journal of Marine and Freshwater Research 35 (2), 343–362.

O'Reilly, J.E., et al., 2000. SeaWiFS Postlaunch Calibration and Validation Analyses, Part 3. NASA Tech. Memo. 2000-206892. In: Hooker, S.B., Firestone, E.R. (Eds.), NASA Goddard Space Flight Center, Vol. 11, 49pp.

O'Reilly, J.E., Maritorena, S., Mitchell, D.G., Siegel, D.A., Carder, K.L., Garver, S.A., Karhu, M., McClain, C., 1998. Ocean color chlorophyll algorithms for SeaWiFS. Journal of Geophysical Research 103, 24937–24953.

Peterson, R.G., Stramma, L., 1991. Upper-level circulation in the South Atlantic Ocean. Progress Oceanography 26, 1–73.

Richardson, M.J., Weatherly, G.L., Gardner, W.D., 1993. Benthic storms in the Argentine Basin. Deep-Sea Research II 40 (4–5), 975–987.

Siddorn, J.R., Bowers, D.G., Hoguane, A.M., 2001. Detecting the Zambezi River plume using observed optical properties. Marine Pollution Bulletin 42 (10), 942–950.

Siegel, D.A., Dickey, T.D., Washburn, L., Hamilton, M.K., Mitchell, B.G., 1989. Optical determination of particulate

abundance and production variations in the oligotrophic ocean. Deep-Sea Research 36 (2), 211–222.
SIO Report, 1992. South Atlantic Ventilation Experiment (SAVE) Chemical, Physical, and CTD data report. Leg 1, 23 November 1987–13 December 1987; Leg 2, 18 December 1987–23 January 1988; Leg 3, 29 January 1988–7 March 1988. *R/V Knorr*. Scripps Inst. of Oceanography, La Jolla, CA (USA). Oceanographic Data Facility. SIO Ref. Ser. Scripps Inst. Oceanography, no. 92–9, 1992, 729pp.
Stramski, D., Reynolds, R.A., Kahru, M., Mitchell, B.G., 1999. Estimation of particulate organic carbon in the ocean from satellite remote sensing. Science 285 (5425), 239–242.
Taylor, A.H., Watson, A.J., Robertson, J.E., 1992. The influence of the spring phytoplankton bloom on carbon dioxide and oxygen concentrations in the surface waters of the northeast Atlantic during 1989. Deep-Sea Research 39, 137–152.
Thomas, A.C., Blanco, J.L., Carr, M.E., Strub, P.T., Osses, J., 2001. Satellite-measured chlorophyll and temperature variability off northern Chile during the 1996–1998 La Niña and El Niño. Journal of Geophysical Research-Oceans 106 (C1), 899–915.
Toole, D.A., Siegel, D.A., 2001. Modes and mechanisms of ocean color variability in the Santa Barbara Channel. Journal of Geophysical Research-Oceans 106 (C11), 26985–27000.
Wood, M.M., 1993. Particulate matter in the South Atlantic Ocean. Ms. Sc. in Oceanography Thesis. Department of Oceanography, Texas A&M University, May 1993, 85pp.
Zaneveld, J.R.V., 1973. Variation of optical sea parameters with depth. In: Optics of the Sea (Interface and In-Water Transmission and Imagery). NATO Lecture Ser., Vol. 61, 2.3-1–2.3-22.